

MICROWAVE COMPLEX PERMITTIVITIES OF Si AND GaAs AT HIGH  
ELECTRIC FIELDS, AND GUNN INSTABILITIES AT VARIOUS  
TEMPERATURES AND MAGNETIC FIELDS.

---

A THESIS SUBMITTED IN PARTIAL FULFILLMENT OF THE  
REQUIREMENTS FOR THE DEGREE OF

MASTER OF SCIENCE

IN THE DEPARTMENT OF ELECTRICAL ENGINEERING  
UNIVERSITY OF MANITOBA

BY

SING - MAN WU

MAY, 1970



## ACKNOWLEDGEMENT

The author wishes to express his grateful appreciation to Dr. K.C. Kao for suggesting the thesis subject and for his supervision throughout the entire work, to Professor E. Bridges for his guidance and assistance in instrumentation and his deep interest in the project.

Sincere thanks must be given to the University of Manitoba and the National Research Council of Canada for awards of scholarships which allowed the author to do this work. The research was supported by the National Research Council through the research grants made to Dr. K.C. Kao.

Valuable technical help given by Mr. R. Woods and Mr. Trider's office is gratefully acknowledged.

The author also wishes to thank Mr. H.C. Law for his interest in the project and many fruitful discussions.

ABSTRACT

A method for measuring the microwave complex permittivity of a semiconductor is described. Measurements have been made on both n-Si and n-GaAs at room and near liquid nitrogen temperatures. Results of measurements at 9.03 GHz with applied field up to 4.5 kV/cm are given and semiquantitatively analysed using a momentum relaxation time to describe various scattering mechanisms.

Gunn instabilities have also been investigated under various environmental conditions. Results show that the natural characteristics of the instabilities such as threshold field and frequency are not appreciably affected by the ambient temperature, while application of a transverse magnetic field has the effect of increasing the amplitude of the instabilities when the sample is biased at threshold, but reduces them at higher bias fields.

TABLE OF CONTENTS

## Chapter I. INTRODUCTION

- |     |   |   |
|-----|---|---|
| 1.1 | Complex permittivity of semiconductors      | 1 |
| 1.2 | Complex permittivity and high field effects | 2 |

## Chapter 2. REVIEW OF PREVIOUS RELATED WORK

- |       |   |    |
|-------|---|----|
| 2.1   | Introduction  | 5  |
| 2.2   | Microwave permittivity of semiconductors in the presence of a high dc field | 6  |
| 2.2.1 | Experimental results and observations                                       | 6  |
| 2.2.2 | Theories of hot-carrier microwave conduction                                | 13 |
| 2.3   | Basic aspects of the Gunn effect  | 23 |
| 2.3.1 | The electron transfer mechanism   | 23 |
| 2.3.2 | The velocity-field (v-E) characteristics and domain formation               | 27 |
| 2.3.3 | Conditions for a disturbance to grow to a stable configuration              | 30 |

## Chapter 3. MEASUREMENT OF MICROWAVE COMPLEX PERMITTIVITY OF A SEMICONDUCTOR SUBJECTED TO A HIGH dc FIELD

- |     |  |    |
|-----|--|----|
| 3.1 | Introduction   | 35 |
| 3.2 | The magnetic Hertzian potential  | 36 |
| 3.3 | Rectangular waveguide loaded centrally with an infinite semiconductor slab | 37 |

	IV
3.4 Propagation constant of the loaded guide	40
3.5 Effect of the slots	43
3.6 Computations	44
Chapter 4. EXPERIMENTAL PROCEDURES	
4.1 Preparation of samples	47
4.2 Application of external bias field	48
4.3 Measurement of microwave complex permittivity at high bias electric fields	49
4.3.1 Description of the circuit and apparatus	49
4.3.2 Measuring procedures	55
4.3.3 Sources of errors	56
4.4 Measurements of Gunn instabilities	57
Chapter 5. RESULTS	
5.1 Microwave complex permittivities of silicon and gallium arsenide as functions of bias field	59
5.1.1 N-type silicon	59
5.1.2 N-type gallium arsenide	65
5.2 Gunn instabilities	71
5.2.1 The effect of input pulse shape	71
5.2.2 The effect of temperature and illumination	73
5.2.3 The effect of transverse magnetic field	75
Chapter 6. ANALYSIS OF RESULTS AND DISCUSSION	
6.1 Resistivity and dielectric constant	77

6.1.1	Microwave resistivity and dielectric constant	77
6.1.2	Microwave resistivity and dielectric constant at high electric fields	78
6.2	Gunn instabilities	85
Chapter 7. CONCLUSION		92
BIBLIOGRAPHY		94
Appendix A. OHMIC CONTACTS ON GaAs AND Si		102
A.1	Introduction	102
A.2	Evaporated ohmic contacts on GaAs	103
A.3	Evaporated ohmic contacts on Si	107
Appendix B. THE HIGH VOLTAGE PULSE GENERATOR		
B.1	Introduction	108
B.2	Principles of operation	108
B.3	The pulse generator	109
B.4	Performance	111
Appendix C. COMPUTER PROGRAMS		113

LIST OF MOST USED SYMBOLS

- a Width of waveguide (p. 37)
- A Attenuation (p. 42, Eqn. 3-28)
- $\vec{A}$  Magnetic vector potential (p. 36)
- b Height of waveguide (p. 37)
- $\vec{B}$  Magnetic flux density (p. 36)
- $C_L$  Mass density X square of longitudinal sound velocity, i.e.,  
average longitudinal elastic constant (p. 80)
- d Sample width (p. 41)
- $\vec{D}$  Electric displacement vector (p. 1)
- e Electronic charge; base of natural logarithm
- $E, E^*$  Electric field (pp. 1, 20)
- $E_0, E_0^*$  Bias field (pp. 20, 30)
- $E_0$  Effective field determining the strength of carrier coupling  
to polar modes (p. 81)
- $E_L$  Magnitude of ac field intensity (p. 1); acoustic deformation  
potential constant (p. 80)
- $E_D$  Domain field (p. 27)
- $E_P$  Peak field (p. 87)
- $E_T$  Threshold field (p. 27)
- $E_U$  Field outside domain in uniform material of Gunn diode (pp. 27, 29)
- $\mathcal{E}$  Carrier energy (p. 15)
- $\mathcal{E}_L$  Thermal equilibrium energy of carriers (p. 15)
- $E_x^c$  Field intensity at contact (p. 89)

ETM	Electron transfer mechanism (p. 23)
$f$	Distribution function of carriers (pp. 17, 18)
$f_o$	Spherically symmetric part of distribution (p. 18)
$f_e, g_e$	Factors in drift term of distribution (pp. 18, 19)
$f_{os}$	Time independent part of $f_o$ (p. 20)
$f_1$	Factor in time dependent term of $f_o$ (p. 20)
$g_{es}$	Time independent part of $g_e$ (p. 20)
$g_1$	Factor in time dependent term of $g_e$ (p. 20)
$h$	Planck's constant
$\hbar$	$= h/(2\pi)$
$\vec{H}$	Magnetic field intensity (p.1)
HFD	High field domain (p. 29)
$j$	Complex number $= \sqrt{-1}$ (p. 1)
$J$	Current density (p. 1)
$J_T$	Total current density (p. 29)
$k_B$	Boltzmann's constant (p. 5)
$k$	Space constant (wave number) (pp. 1, 31)
$k_E$	Component of electron wave vector ( $k$ ) in the field direction (p. 19)
$k_o$	Free space wave number (p. 36)
$L$	Sample length (p. 29)
$m^*$	Effective mass (p. 19)
$m_o$	Rest mass of electron (pp. 24, 79)
$m_D$	Density of state mass (p. 17)
$n$	Available electron concentration (pp. 16, 29)
$N$	Impurity concentration, if fully ionized, equals concentration of available electrons insuring electrical neutrality (p. 30)



- NDR Negative differential resistance (p. 23)
- $N_q$  Number of longitudinal optical phonons given by the Bose-Einstein statistics (p. 81)
- r Normalized load resistance (p. 33)
- R Resistance (p. 37)
- S Entropy (p. 86)
- t Time (p. 14); thickness of semiconductor slab (p. 37)
- T Absolute temperature (p. 5)
- $T_e$  Effective carrier temperature (p. 5)
- $T_o$  Period (p. 29)
- $\hat{T}$  Transmission coefficient (p. 42)
- u Unit step function (p. 109)
- v Carrier drift velocity (pp. 7, 30); displaced velocity in displaced Maxwellian distribution function (p. 17)
- $v_D$  Domain drift velocity (p. 85)
- $v_P$  Peak velocity (p. 85)
- $v_U$  Drift velocity in uniform material outside HFD (pp. 29, 85)
- $v_o$  Drift velocity in bias field  $E_o$  (pp. 29, 31)
- V Free carrier velocity (p. 17); abbreviation for 'volt'
- $V_o$  Charged voltage (p. 109)
- x Coordinate axis; dimensionless parameter =  $\frac{\mathcal{E}}{\hbar\omega_e}$  (p. 83)
- $x_o$  Dimensionless quantity =  $\frac{\hbar\omega_e}{k_B T}$  (p. 83)
- $\hat{z}$  complex variable (p. 46)
- $\hat{Z}$  Wave impedance of loaded guide (p. 41)
- $\hat{Z}_o$  Characteristic impedance of empty guide (p. 41)

$\alpha$	Real part of $\hat{\gamma}$ (p. 40)
$\beta$	Imaginary part of $\hat{\gamma}$ (p. 40)
$\Delta E$	Energy difference between (000), (100) minima of conduction band of GaAs. (p. 26)
$\Delta E_G$	Band gap of a semiconductor (p. 26)
$S E$	Constant parameter (p. 84)
$\delta$	Skin depth (p. 47)
$\gamma$	Constant (p. 83)
$\hat{\gamma}$	Propagation constant (p. 38)
$\Pi$	a parameter (P. 16, Eqn 2-16)
$\vec{\Pi}_h$	Magnetic Hertzian potential (p. 36)
$\mu$	Mobility (pp. 79, 89)
$\mu_{ac}$	Small signal mobility (p. 8)
$\mu_{dc}$	dc mobility (pp. 8, 16)
$\mu_{do}$	Differential mobility at bias field $E_o$ (p. 31)
$\mu_o$	Free space permeability (p. 36)
$\rho$	Resistivity (. 40)
$\hat{\rho}$	Interfacial reflection coefficient (p. 42)
$\sigma$	Real part of complex conductivity $\sigma = \sigma_R$ (p. 2)
$\hat{\sigma}$	Complex conductivity (p. 2)
$\tau_a$	Relaxation time for acoustic phonon scattering (p. 80)
$\tau_E$	Energy relaxation time (p. 15)
$\tau_m$	Momentum relaxation time (p. 15)
$\tau_{po}$	Relaxation time for polar optical scattering (p. 83)
	Interfacial transmission coefficient (p. 42)

$\epsilon$	Real part of complex permittivity, i.e., dielectric constant (p. 2)
$\epsilon^*$	Complex permittivity of an insulator $\epsilon^* = \epsilon - j\epsilon''$ (p. 1)
$\epsilon_t^*$	Total complex permittivity $\epsilon_t^* = \epsilon - j(\epsilon'' + \frac{\sigma}{\omega})$ (p. 2)
$\hat{\epsilon}$	Complex permittivity of a semiconductor $\hat{\epsilon} = \epsilon - j\frac{\sigma}{\omega}$ (p. 2)
$\epsilon_0$	Free space permittivity = $8.854 \times 10^{-14}$ farad/cm (p. 36); dielectric constant at zero frequency (p. 82)
$\epsilon_\infty$	Dielectric constant at infinite frequency (p. 82)
$\hat{\epsilon}_r$	Complex relative permittivity (p. 38)
$\epsilon_r$	Relative dielectric constant = $\epsilon/\epsilon_0$ (p. 38)
$\epsilon_r'$	Imaginary part of complex relative permittivity $\epsilon_r' = \frac{\sigma}{\omega\epsilon_0}$ (p. 38) Phase change (P. 42, Eqn. 3-28)
$\Phi_B$	Bias voltage for a Gunn diode (p. 29)
$\Phi_D$	Domain excess voltage (p. 29)
$\Phi$	Scalar function (p. 36)
$\psi$	Factor in magnetic Hertzian potential function (p. 38)
$\omega$	Angular frequency (p. 1)
$\omega_l$	Angular frequency of longitudinal phonons (p. 82)
$\Omega$	A parameter (p. 16, Eqn. 2-13); abbreviation for 'ohm'

## CHAPTER 1

## INTRODUCTION

1.1 COMPLEX PERMITTIVITY OF SEMICONDUCTORS

The permittivity or dielectric constant  $\epsilon$  of a lossless material, as firstly conceived by M. Faraday, is a parameter which relates the displacement  $\vec{D}$  and field strength  $\vec{E}$  at the point in question according to the relation

$$\vec{D} = \epsilon \vec{E} \quad 1-1$$

If the material is lossy, yet there is no conduction loss ( $\sigma = 0$ ), one finds that its permittivity is necessarily a complex quantity, since its imaginary part can then account for the rate of production of Joule heat in the real part of  $\vec{J} \cdot \vec{E}$ , where  $\vec{J}$  is the current density at the point in question. Thus one formally writes  $\epsilon^* = \epsilon - j\epsilon''$  for the complex permittivity and  $\epsilon''$  accounts for losses due to frictional motion of bound charges. For a nonmagnetic material,  $\vec{J}$  is given by the right side of the following Maxwell equation in M.K.S. units

$$\nabla \times \vec{H} = \epsilon^* \frac{\partial \vec{E}}{\partial t} + \sigma \vec{E} \quad 1-2$$

For a field

$$\vec{E} = \vec{E}_1 e^{j(\vec{k} \cdot \vec{r} + \omega t)} \quad 1-3$$

one has

$$\begin{aligned} \vec{J} &= (j\omega\epsilon^* + \sigma) \vec{E} \\ &= \left[ \epsilon - j(\epsilon'' + \frac{\sigma}{\omega}) \right] j\omega \vec{E} \end{aligned} \quad 1-4$$

If one equates the right hand side of Eqn. 1-4 to  $\frac{\partial \vec{D}}{\partial t}$ , one then automatically defines a total complex permittivity  $\epsilon_t^*$  given by\*

$$\epsilon_t^* = \epsilon - j\left(\epsilon'' + \frac{\sigma}{\omega}\right) = \epsilon - j\epsilon' \quad 1-5$$

For semiconductors in the microwave frequency region,  $\frac{\sigma}{\omega}$  is much greater than  $\epsilon''$ , hence  $\epsilon_t^*$  is generally called the complex permittivity of a semiconductor and denoted by

$$\hat{\epsilon} = \epsilon - j\frac{\sigma}{\omega} \quad 1-6$$

This designation is employed here-after in this thesis.

## 1.2 COMPLEX PERMITTIVITY AND HIGH FIELD EFFECTS

From Eqn. 1-6, one notices that the complex permittivity is not independent of conductivity; in fact, this same parameter is sometimes characterized by defining a complex conductivity given by

$$\hat{\sigma} = \sigma + j\omega\epsilon \quad 1-7$$

so that the Maxwell equation  $\nabla \times \vec{H} = \hat{\sigma} \vec{E}$  is satisfied. In spite of various notations,  $\epsilon$  and  $\sigma$  remain as important parameters characterizing the interaction of a material with an electromagnetic field. Studies of high field phenomena in semiconductors generally involve observing the

---

\* Sometimes  $\epsilon^*$  is written as  $\epsilon^* = \epsilon + j\epsilon''$ ; if so,  $\epsilon_t^*$  is given by  $\epsilon_t^* = \epsilon^* + j\frac{\sigma}{\omega}$ ; this representation arises from the choice of  $e^{-j\omega t}$  dependence of the  $\vec{E}$  field instead of  $e^{+j\omega t}$ .

variations of the permittivity parameters as the applied field is increased, keeping the carrier density constant. Extensive studies have been done on germanium, contributing significantly to the understanding of the nature of this material. Currently according to Conwell (1967), the behaviour of electrons at room temperature in germanium can be accounted for quantitatively up to energies as high as ten times thermal, or fields of about 5 kV/cm.

The study of high field transport in semiconductors is of considerable practical importance because many solid state electronic devices are either based on some effects of high fields on carriers, or necessarily involve them in their operation. In spite of the fact that silicon is no less an important material in semiconductor technology than germanium, experimental and theoretical high field studies have been much less extensive for silicon than for germanium. Because of this fact, the present investigation on silicon was carried out.

Studies of high field effects on n-GaAs have been most fruitful. Gunn, in 1963, looking for a non-linearity in the current voltage characteristic of n-GaAs, applied high voltage pulses to his samples and found that when the field inside the material was raised above a threshold value, the current waveform oscillated with a frequency in the range of microwave frequencies. This phenomenon was subsequently called the "Gunn effect". This effect has potential applications in the electronic industry, especially in the field of microwave technology (Thim et al 1965, and Dow et al 1966). Since Gunn effect devices are based on the effects of high fields on carriers, it is naturally desirable to investigate the complex permittivity

of the material concerned at microwave frequencies under operational conditions. For the sake of Gunn effect alone, it is practical as well as interesting to investigate current instabilities under various environmental conditions; not merely because such investigations may lead to a better understanding of the phenomenon but also because device performance may be improved by tailoring environment.

In the light of previous discussions, it is therefore the purpose of this thesis to present a method for the measurement of the complex permittivity of a semiconductor subjected to a high dc electric field at microwave frequencies. Measurements on both n-Si and n-GaAs were carried out at room as well as at near liquid nitrogen temperatures. Gunn instabilities were also studied under various environmental conditions such as low temperature, illumination, and placing the sample in a transverse magnetic field.

## CHAPTER 2

## REVIEW OF PREVIOUS RELATED WORK

2.1 INTRODUCTION

Early studies of high field effects on solids are associated with insulators and the problem of dielectric breakdown (Fröhlich and Seitz 1950). Actually, semiconductors are best suited for such studies because unlike insulators, charge carriers are present in the absence of applied fields, hence their behaviour can be traced as their average energy is increased by the field. Also, unlike metals, the mean energy of an electron in a semiconductor is much smaller than that in a metal (Shockley 1951a), so that high field phenomena arising from carrier energy variations may most readily be observed. Realizing these facts, Shockley (1951) and Ryder (1953) carried out successfully the first experiment of high field effect on n-type germanium. Their experimental technique and theoretical work laid the foundation for a great deal of further work on "hot electrons<sup>\*</sup>", a term coined for high energy electrons. To-day, high field transport in semiconductors has become an important branch in solid state physics.

---

\* Under the assumption of Maxwellian distribution, the mean energy of an electron is  $(3/2)k_B T$  where  $T$  is the equilibrium temperature of the lattice and  $k_B$  the Boltzmann constant. If an electron gains energy from the field, an effective temperature  $T_e$  can be defined such that electron energy =  $(3/2)k_B T_e$ . Since  $T_e > T$ , the electron is called a hot electron.



## 2.2 MICROWAVE PERMITTIVITY OF SEMICONDUCTORS IN THE PRESENCE OF A HIGH dc FIELD

### 2.2.1 EXPERIMENTAL RESULTS AND OBSERVATIONS

One of the early experiments employing microwaves to study the absorption properties of semiconductors subjected to a high dc field is that of Arthur et al (1956). In their experiment, the semiconductor sample is cut in the form of a rectangular slab and inserted into the waveguide through narrow slots cut in the centre of the broad faces of the guide. The dc field is applied parallel to the microwave field. With a 5 ohm-cm n-germanium sample, they found that microwave attenuation decreases with increasing applied dc field. Also since the dc field is parallel to the microwave field and since the latter is much smaller than the former, they argued that the field due to the microwave radiation represents a small oscillation around the mean applied field so the absorption is proportional to the differential mobility at that applied field (the microwave frequency used corresponds to a wavelength of 8 mm). Based on this argument, they obtained a graph (Fig. 1) showing the electron velocity as a function of applied external field. Hence a saturation velocity at around 4.5 kV/cm was obtained, in general agreement with Ryder (1953) and Shockley (1951).

Employing the same sample waveguide geometry as that of Arthur et al, Gibson et al (1961) measured at room temperature the attenuation and phase shift (at frequency of 34.75 GHz) due to a germanium sample under various dc fields. After deducing the mobility and dielectric constant from these measurements they found, (1) that the mobility at the

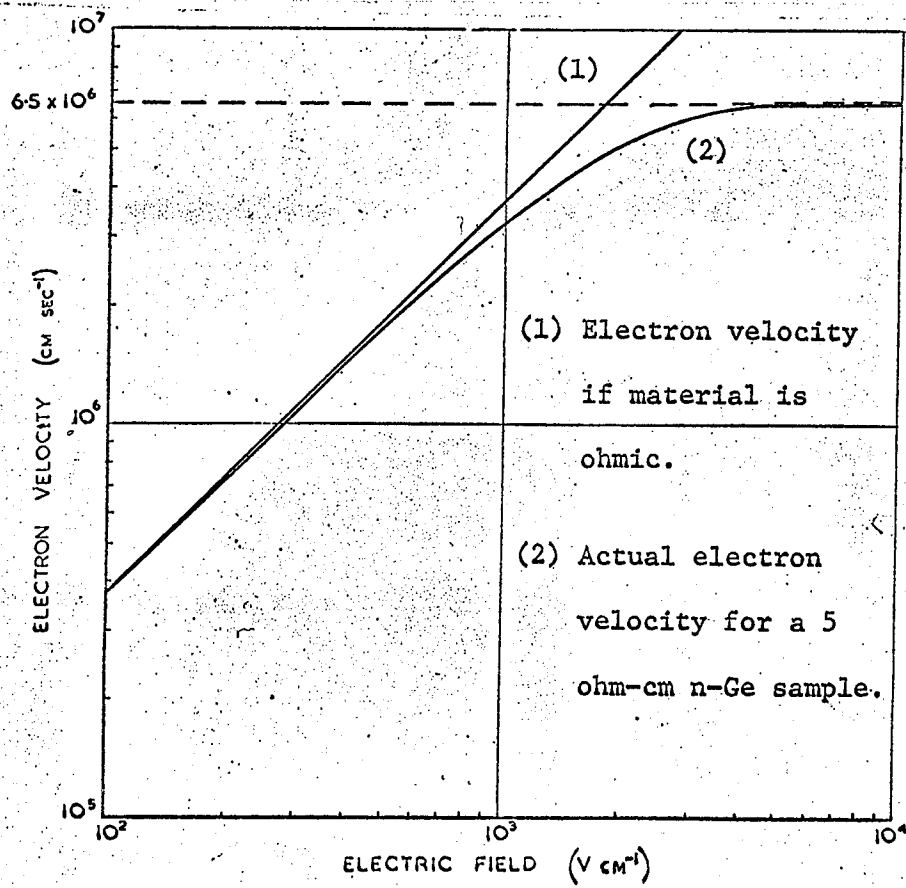


Fig. 1. Variation of electron velocity with electric field for a 5 ohm-cm n-germanium sample. (After Arthur et al 1956).

microwave frequency employed is intermediate between the mobility ( $v/E$ ) and the differential mobility ( $dv/dE$ ) obtained from the variation of carrier velocity with electric field, and (2) that the contribution of the free carriers to the dielectric constant is negative at zero field but becomes positive at higher fields. Their theory relating mobility and dielectric constant is found to be obeyed by electrons (Fig. 3) but not by holes. Their results for n-germanium are shown in Figs. 2 and 3.

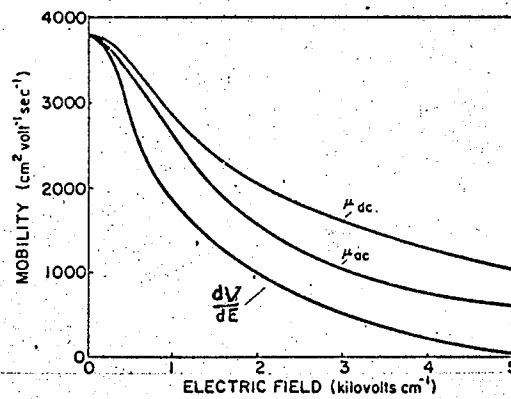


Fig. 2. Experimental values of dc mobility, small-signal (35 GHz) mobility  $\mu_{ac}$  and  $dV/dE$  versus  $E_{dc}$  for an n-germanium sample with low-field resistivity 4.7 ohm-cm at 300°K (After Gibson et al 1961).

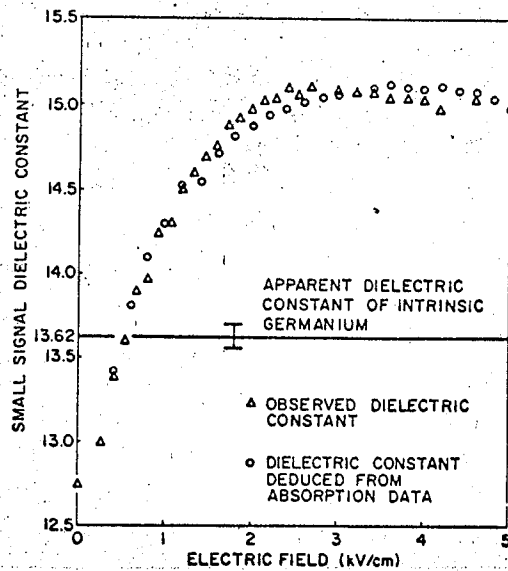


Fig. 3. Small-signal (35 GHz) dielectric constant versus dc bias field for the n-germanium sample used for Fig. 2. (After Gibson et al 1961).

Another experiment of the type involving the heating of charge carriers by large dc pulses and superimposing on these a small microwave signal parallel to the dc field for the determination of the semiconductor complex permittivity is that of Conwell et al (1962/63, see also Conwell 1967, pp 39-45). In this experiment, the sample is shaped in the form of a thin filament (thin compared to the skin depth) and introduced through small circular slots cut in the broad faces of the waveguide. The guide is shorted at one quarter of a guide wavelength beyond the sample. By measuring the complex reflection coefficient of such a system, they were able to deduce the impedance of the semiconductor wire and hence its complex permittivity. The variations of conductivity and dielectric constant at a measuring frequency of 70 GHz for moderately doped n-germanium samples are shown in Figs. 4 and 5. More detailed measurements revealed that the field dependence of conductivity and dielectric constant of n-germanium depends also on the crystal orientation. Data showing the small signal conductivity versus dc bias taken along different crystal directions is not available; since the dc results represent a close approximation, the dc conductivity and the small signal dielectric constant as functions of bias fields taken along different crystal orientations and at liquid nitrogen temperature are given in Figs. 6 and 7. While it is observed that the effect of crystal anisotropy on conductivity is maximum at about 1 kV/cm, and decreases at higher fields; generally, the conductivity decreases monotonically with increasing fields. The small signal dielectric constant, on the other hand, increases with electric field to a maximum value before it decreases again. The phenomenon of anisotropy has also been observed in n-silicon (Hamaguchi and Inuishi 1966).

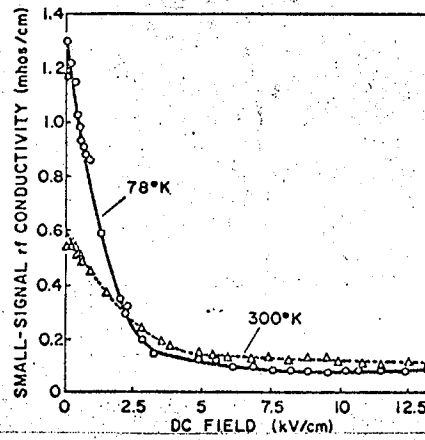


Fig. 4. Small-signal (70 GHz) conductivity versus dc bias field for an n-germanium sample with 300°K low-field resistivity of 1.9 ohm-cm. (After Conwell 1967).

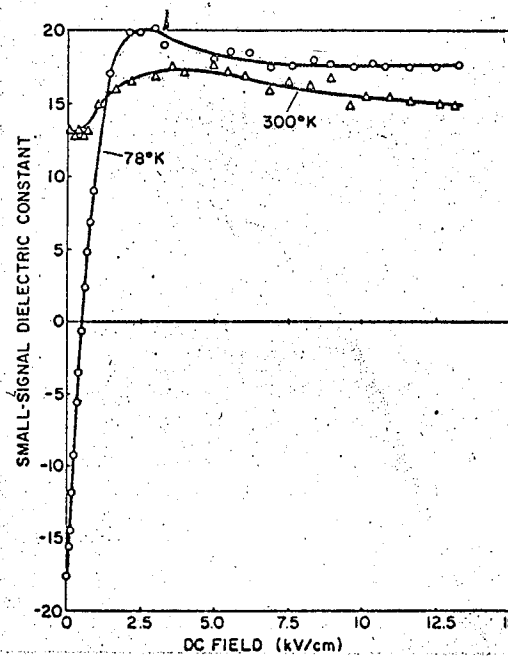


Fig. 5. Small-signal (70GHz) dielectric constant versus dc bias field for the same sample used for Fig. 4. (After Conwell 1967).